

1     **The Unique Evolutionary Trajectory and Dynamic Conformations of DR and IR/DR-**  
2             **coexisting Plastomes of the Early Vascular Plant Selaginellaceae (Lycophyte)**

3     Hong-Rui Zhang<sup>1,2</sup>, Qiao-Ping Xiang<sup>1\*</sup>, Xian-Chun Zhang<sup>1\*</sup>

4     <sup>1</sup> State Key Laboratory of Systematic and Evolutionary Botany, Institute of Botany, the  
5     Chinese Academy of Sciences, Beijing 100093, China.

6     <sup>2</sup> University of Chinese Academy of Sciences, Beijing 100049, China.

7     **\*Author for Correspondence:** Qiao-Ping Xiang, Email: [qpxiang@ibcas.ac.cn](mailto:qpxiang@ibcas.ac.cn)

8                                     Xian-Chun Zhang, Email: [zhangxc@ibcas.ac.cn](mailto:zhangxc@ibcas.ac.cn)

9     **Data deposition:** All the plastomes were deposited in GenBank under accession  
10    numbers MG272483-MG272484, MH598531-MH598537 and MK156800.

11

12

13

14

15

16

17

18

19

20

21

22

23

24 **Abstract**

25 Both direct repeats (DR) and inverted repeats (IR) are documented in the published  
26 plastomes of four *Selaginella* species indicating the unusual and diverse plastome  
27 structure in the family Selaginellaceae. In this study, we newly sequenced complete  
28 plastomes of seven species from five main lineages of Selaginellaceae and also re-  
29 sequenced three species (*S. tamariscina*, *S. uncinata* and *S. moellendorffii*) to explore  
30 the evolutionary trajectory of Selaginellaceae plastomes. Our results showed that the  
31 plastomes of Selaginellaceae vary remarkably in size, gene contents, gene order and  
32 GC contents. Notably, both DR and IR structure existed in the plastomes of  
33 Selaginellaceae with DR structure being an early diverged character. The occurrence  
34 of DR structure was right after the Permian-Triassic (P-T) extinction (ca. 246 Ma) and  
35 remained in most subgenera of Selaginellaceae, whereas IR structure only reoccurred  
36 in the most derived subg. *Heterostachys* (ca. 23 Ma). The presence of a pair of large  
37 repeats *psbK-trnQ*, together with DR/IR region in *S. bisulcata*, *S. pennata*, *S. uncinata*,  
38 and *S. hainanensis*, could frequently mediate diverse homologous recombination and  
39 create approximately equal stoichiometric isomers (IR/DR-coexisting) and  
40 subgenomes. High proportion of repeats is presumably responsible for the dynamic  
41 IR/DR-coexisting plastomes, which possess a lower synonymous substitution rate (dS)  
42 compared with DR-possessing plastomes. We propose that the occurrence of DR  
43 structure, together with few repeats, is possibly selected to adapt to the  
44 environmental upheaval during the P-T crisis and the IR/DR-coexisting plastomes also  
45 reached an equilibrium in plastome organization through highly efficient homologous  
46 recombination to maintain stability.

47 **Keywords:** gene loss; DR/IR evolution; homologous recombination; *Selaginella*;  
48 substitution rate; time divergence

49

## 50 Introduction

51 Plastid genomes (plastomes) of almost all land plants are highly conserved and present  
52 the canonical quadripartite structure with a pair of large inverted repeats (termed IR<sub>A</sub>  
53 and IR<sub>B</sub>) separated by two single copy regions (termed LSC and SSC) (Mower and  
54 Vickrey 2018). Normally, the range of the IR varies through expansion or contraction.  
55 Complete loss of the IR is rare but has been observed in some species of Fabaceae (Cai  
56 et al. 2008; Lavin et al. 1990), Geraniaceae (Blazier et al. 2016; Guisinger et al. 2011;  
57 Ruhlman et al. 2017), and Cactaceae (Sanderson et al. 2015). Remarkably, plastomes  
58 with a pair of large direct repeats (termed DR<sub>A</sub> and DR<sub>B</sub>) have been documented for  
59 two species of Selaginellaceae, *Selaginella tamariscina* (Xu et al. 2018) and *S. vardei*  
60 (Unpublished data) in land plants. The DR structure in Selaginellaceae was explained  
61 to have occurred by ca. 50 kb fragment inversion with a complete IR<sub>B</sub> being included,  
62 compared with the plastome of its sister family Isoetaceae (Unpublished data).

63 In addition to the exceptional existence of plastomes with DR structure, a salient  
64 fraction of land plants plastomes experienced significant structural rearrangements,  
65 with evidence of large inversions and loss of entire gene family, despite the overall  
66 conservation in structures and gene order (Mower and Vickrey 2018). A 30 kb inversion  
67 (*ycf2-psbM*) was detected in the large single copy (LSC) of ferns and seed plants  
68 plastomes relative to bryophytes and lycophytes, which is a strong evidence showing  
69 lycophytes are located at the basal position of vascular plants (Raubeson and Jansen  
70 1992). The plastomes of ferns underwent two hypothetical inversions (CE inversion  
71 (*trnC* to *trnE*) and DE inversion (*trnD-trnY*)) within *rpoB-psbZ* (BZ) region from the  
72 ancestral gene order in eusporangiates to the derived gene order in core  
73 leptosporangiates whereas the plastome structures within these two groups were  
74 generally consistent, respectively (Gao et al. 2013; Gao et al. 2011; Grewe et al. 2013).  
75 Many other rearrangements also exist in some conifers (Chaw et al. 2018) and several  
76 angiosperm lineages like Campanulaceae, Fabaceae, and Geraniaceae (Mower and  
77 Vickrey 2018; Ruhlman and Jansen 2018). Inversion facilitated by recombination,  
78 transposition, and expansion/contraction of the IR have been suggested as three

79 different mechanisms that cause rearrangements in land plants (Jansen and Ruhlman  
80 2012). However, it is recently recognized that most plastomes exists as  
81 linear/concatemeric/highly branched complex molecules in plants and these  
82 rearrangement events are reinterpreted as result of a BIR-like, recombination-  
83 dependent replication mechanism between different linear plastome templates  
84 (Oldenburg and Bendich 2015). Furthermore, four families of nuclear-encoded  
85 proteins (MutS homologue 1 (*MSH1*), RecA-like recombinases, the organellar ssDNA-  
86 binding proteins (*OSBs*), and the Whirlies) have been characterized to target to both  
87 mitochondria and plastid, or some protein members of the four families target to only  
88 plastids and function as recombination surveillance machinery in plant plastids  
89 (Maréchal and Brisson 2010).

90 Gene and intron content are highly conserved among the vast majority of land plants  
91 plastomes, however, numerous examples of gene loss or pseudogenization have been  
92 identified in several angiosperm lineages (Ruhlman and Jansen 2014). For example,  
93 most or all of the suite of 11 functionally related *ndh* genes have been lost  
94 independently in a small assortment of taxa with diverse habitat, including the  
95 parasitic *Epifagus* (Wicke et al. 2011), the mycoheterotrophic *Rhizanthella gardneri*  
96 (Delannoy et al. 2011), some members of the carnivorous Lentibulariaceae (Wicke et  
97 al. 2013), the xerophytic *Saguaro cactus* (Sanderson et al. 2015) and gnetales  
98 (Braukmann et al. 2009), the aquatic *Najas flexilis* (Peredo et al. 2013) and some taxa  
99 with less unusual life histories, such as Pinaceae (Braukmann et al. 2009) and *Erodium*  
100 (Blazier et al. 2011a). In addition, the loss of protein coding genes and tRNA genes has  
101 occurred sporadically in different land plants lineages (Ruhlman and Jansen 2014; Wu  
102 and Chaw 2015). The fatty acid synthesis related gene, *accD*, has been lost from  
103 plastomes of angiosperm at least seven times (Jansen et al. 2007). Similarly, more than  
104 a dozen parallel losses of ribosomal protein (*rps/rpl*) gene have occurred in different  
105 lineages of land plants (Ruhlman and Jansen 2014). Three major pathways of gene loss  
106 have been detected in land plants: (1) gene transfer to the nucleus (*infA*, *rpl22*, *rpl32*  
107 and *accD*), (2) substitution by a nuclear-encoded, mitochondrial targeted gene product

108 (*rps16*), and (3) substitution by a nuclear-encoded protein for a plastid gene product  
109 (*accD*, *rpl23*) (Jansen and Ruhlman 2012). The multiple independent *ndh* gene loss in  
110 different lineages is supposed to belong to the third pathway (Ruhlman et al. 2015).

111 Selaginellaceae, one of the most ancient vascular plants with nearly 400 million years  
112 of evolutionary history (Banks 2009), is the largest family of lycophytes with ca. 750  
113 species classified into the only genus *Selaginella* (Jermy 1990; Weststrand and Korall  
114 2016b; Zhou et al. 2016). *Selaginella* species have highly diverse growth forms,  
115 including creeping, climbing, prostrate, erect and rosetted forms, and also inhabit an  
116 impressive range of habitats, from tropical rain forests to deserts, alpine and arctic  
117 habitats (Zhang et al. 2013). With such a high diversity in habitat and growth forms,  
118 complex plastomes with different structures are expected in Selaginellaceae (Tsuji et  
119 al. 2007). However, only four species of *Selaginella*, viz., *S. uncinata* (Tsuji et al. 2007),  
120 *S. moellendorffii* (Smith 2009), *S. tamariscina* (Xu et al. 2018), and *S. vardei*  
121 (Unpublished data), have been reported for their plastomes. Compared to the four  
122 species from Lycopodiaceae and Isoetaceae of lycophytes (Guo et al. 2016; Karol et al.  
123 2010; Wolf et al. 2005; Zhang et al. 2017), plastomes of *Selaginella* are, indeed, far less  
124 conserved in both structures and gene contents. Both *S. uncinata* and *S. moellendorffii*  
125 belong to subg. *Stachygynandrum* based on both morphology-based classification  
126 (Jermy 1986) and a recent molecular-based classification (Weststrand and Korall  
127 2016b). However, their plastomes show divergent variation in structure. Several  
128 rearrangements, such as a 20 kb fragment inversion, a 17 kb fragment transposition  
129 and gene duplications, exist in these two species (Smith 2009). The morphology of *S.*  
130 *tamariscina*, belonging to subg. *Stachygynandrum*, and *S. vardei*, belonging to subg.  
131 *Rupestrae* (sensu Weststrand and Korall 2016) (Weststrand and Korall 2016b) are also  
132 quite divergent from *S. uncinata* and *S. moellendorffii* in having rosetted plant and  
133 helically-arranged trophophylls, respectively. These two species both grow in  
134 extremely xeric habitat. Plastomes with DR rather than IR have been characterized in  
135 *S. tamariscina* (Xu et al. 2018) and *S. vardei* (Unpublished data) was characterized.  
136 Some other features of these plastomes are also quite distinctive. Only 9-12 different

137 tRNA genes remain in *Selaginella*, and GC content in *Selaginella* plastomes is  
138 significantly higher (54.8% for *S. uncinata*, 51% for *S. moellendorffii*, 54.1% for *S.*  
139 *tamariscina*, and 53.2% for *S. vardei*) than the plastomes of other land plants (less than  
140 43%) (Smith 2009; Tsuji et al. 2007). Such extensive rearrangement events and  
141 extraordinary gene content have never been reported in other lycophytes and fern  
142 families (Guo et al. 2016; Karol et al. 2010; Mower and Vickrey 2018).

143 The divergent variation in structure and gene content exhibited by Selaginellaceae  
144 plastomes make it an ideal family to study the complexity and diversity of plastomes.  
145 Furthermore, the extent of genomic change in other lineages of *Selaginella* species  
146 has not been fully investigated. Therefore, we sequenced a total of ten plastomes from  
147 species belonging to six different main lineages of Selaginellaceae using next  
148 generation sequencing and combined previously published plastomes of lycophytes  
149 to reach the following goals: 1) document plastome characteristics from major  
150 lineages of Selaginellaceae, 2) explore the evolutionary trajectory and dynamic  
151 conformations of DR/IR structure in plastomes of Selaginellaceae, and 3) reveal the  
152 potential correlations among plastome rearrangements, substitution rate, and  
153 number of repeats.

154

## 155 **Materials and Methods**

### 156 **Taxon Sampling**

157 Seven taxa (*S. lyallii*, *S. remotifolia*, *S. sanguinolenta*, *S. doederleinii*, *S. pennata*, *S.*  
158 *bisulcata*, and *S. hainanensis*) from five main lineages of Selaginellaceae representing  
159 four subgenera of Zhou and Zhang (2015) and three subgenera of Weststrand and  
160 Korall (2016) were sampled (Table S1). The previously published plastomes of *S.*  
161 *tamariscina*, *S. moellendorffii*, and *S. uncinata* were re-sequenced to confirm their  
162 structures. Previously published plastomes of *S. vardei* (Unpublished data) and four  
163 outgroups from other lycophytes (*Huperzia lucidula* (NC\_006861), *H. javanica*  
164 (KY609860), *H. serrata* (NC\_033874) and *Isoetes flaccida* (NC\_014675))(Guo et al. 2016;  
165 Karol et al. 2010; Wolf et al. 2005; Zhang et al. 2017) were used in the following  
166 analyses. We followed the classification of Zhou and Zhang (2015) to conveniently  
167 describe the lineages represented by our species.

### 168 **DNA Extraction, Sequencing and Assembly**

169 The total genomic DNAs were isolated from silica-dried materials with a modified cetyl  
170 trimethylammonium bromide (CTAB) method (Li et al. 2013). Library construction was  
171 performed with NEBNext DNA Library Prep Kit (New England Biolabs, Ipswich,  
172 Massachusetts, USA) and sequencing was finished by Illumina HiSeq 2500 (Illumina,  
173 San Diego, California, USA). Illumina paired-end reads of each species were mapped to  
174 *S. uncinata* (AB197035) (Tsuji et al. 2007) and *S. moellendorffii* (FJ755183) (Smith 2009),  
175 with medium-low sensitivity in five to ten iterations in Geneious v. 9.1.4 (Kearse et al.  
176 2012)(Biomatters, Inc., Auckland, New Zealand; <https://www.geneious.com>). The  
177 mapped reads were then assembled into contigs in Geneious. We also used bandage  
178 v. 0.8.1 (Wick et al. 2015), a program for visualizing de novo assembly graphs, to help  
179 select contigs of plastome and analyze de novo assemblies by importing the fastg file  
180 created by GetOrganelle (Jin et al. 2018). The contigs obtained from both ways were  
181 then combined and imported into Geneious to extend and assemble into the complete  
182 plastomes.

## 183 **Gene Annotation**

184 Gene annotations were performed with local BLAST (Delsuc et al. 2005) using the  
185 plastomes of *H. serrata* (Guo et al. 2016), *I. flaccida* (Karol et al. 2010), *S. uncinata*  
186 (Tsuji et al. 2007), and *S. moellendorffii* (Smith 2009) as references. Putative start and  
187 stop codons were defined based on similarity with known sequences. The tRNAs were  
188 further verified using tRNAscan-SE version 1.21 (Lowe and Eddy, 1997; Schattner et al.,  
189 2005) and ARAGORN (Laslett and Canback 2004). Circular and linear plastome maps  
190 were drawn in OGDRAW version 1.2 (Lohse et al., 2007).

## 191 **PCR Confirmation of the Plastome Structure of Representative Species in Four** 192 **Subgenera**

193 We selected eighteen representatives (Table S2) from four subgenera to confirm  
194 whether the DR structure is ubiquitous in plastomes of three subgenera and IR  
195 structure only exists in the derived subgenus. Primers were designed at the flank of  
196 rearrangement end points and DR/IR region boundaries. Considering the distant  
197 relationship among these subgenera, we designed the primers (Table S3) for each  
198 subgenus, respectively. The PCR amplifications were performed in a total volume of  
199 25 µL containing 2.5 µL of 10X Ex Taq™ Buffer, 2.5 µL of dNTP Mixture (2.5 mM each),  
200 2 µL of each primer (5 mM), 0.15 µL of TaKaRa Ex Taq™ (5 units/µl) and 20 ng of  
201 template DNA. Cycling conditions were 94 °C for 3 min, followed by 35 cycles of  
202 94 °C for 30 s, 52 °C for 1 min and 72 °C for 1.5 min, and a final extension of 72 °C  
203 for 10 min. The PCR products were verified by electrophoresis in 1% agarose gels  
204 stained with ethidium bromide and sequenced by the Company of Majorbio, Beijing,  
205 China.

## 206 **Plastome Rearrangement Analyses**

207 In order to identify the putative presence of large structural variation within the  
208 *Selaginella* plastomes, whole genome alignment among the 14 lycophyte species  
209 (twelve Selaginellaceae species, *I. flaccida*, and *H. serrata*) was performed using the  
210 progressiveMauve algorithm in Mauve v 2.3.1 (Darling et al. 2010). A copy of DR/IR



211 was removed from the plastomes. The Locally colinear blocks (LCBs) identified by the  
212 Mauve alignment were numbered to estimate the genome rearrangement distances  
213 (Table S4). Genes in each block were also listed (Table S5). Two types of genome  
214 rearrangement distances, break point (BP) and inversions (IVs), were calculated using  
215 the web serve of the Common Interval Rearrangement Explore (CREx) (Bernt et al.  
216 2007) using the conserved plastome of *H. serrata* as a reference.

### 217 **Repeats Analyses**

218 Repeats within the 14 lycophytes plastomes were identified by RepeatsFinder  
219 (Volfovsky et al. 2001) with default parameters (repeat size >15 bp). One copy of the  
220 DR/IR was removed from all plastomes used. The circular layouts of repeats in  
221 plastome were visualized using the *circlize* package (Gu et al. 2014) in R. Furthermore,  
222 the correlation between the number of repeats and the degree of genome  
223 rearrangements, BPs and IVs distance, were tested using Pearson test in R v. 3.4.1 (R  
224 Development Core Team2012).

### 225 **Nucleotide Substitution Rate Analyses**

226 Forty-six protein-coding genes (Table S6) from single copy regions of 12  
227 Selaginellaceae species and one outgroup, *I. flaccida*, were extracted from the  
228 plastomes and aligned at the protein level by MAFFT (Katoh and Standley 2013) using  
229 the translation-aligned function in Geneious v. 9.1.4 (Kearse et al. 2012). Poorly aligned  
230 regions were removed by using Gblocks v. 0.91b (Castresana 2000) with default  
231 parameters. The dataset for substitution rate comparison between plastomes with DR  
232 and IR/DR-coexisting structure in Selaginellaceae includes all twelve *Selaginella*  
233 species. The dataset for comparison of genes inside or outside the ca. 50 kb inversion  
234 (Table S6) includes eight *Selaginella* species with plastomes of DR structure. The  
235 pairwise synonymous substitution rate (dS), nonsynonymous substitution rate (dN),  
236 and dN/dS of each individual gene was estimated using PAML v. 4.9 (run mode=-2)  
237 (Yang 2007) with codon frequencies determined by the F3 × 4 model. The significance  
238 of differences of dS, dN, and dN/dS was assessed using Wilcoxon rank sum tests in R v.

239 3.4.1 (R Development Core Team 2012).

#### 240 **Phylogenetic Analysis and Divergence Time Estimation**

241 Forty-six protein-coding genes (Table S6) with 21,382 bases shared by 16 lycophyte  
242 species (twelve *Selaginella*, one *Isoetes* and three *Huperzia*) were extracted and  
243 aligned using Multiple Alignment in Geneious v. 9.1.4 (Kearse et al. 2012) under the  
244 automatic model selection option with some manual adjustments. The 1<sup>st</sup> and 2<sup>nd</sup> sites  
245 of each codon were selected in MEGA 7.0 (Tamura et al. 2007) to eliminate the effect  
246 of 3<sup>rd</sup> site base substitution saturation. Phylogenetic analysis was performed using  
247 maximum likelihood methods on the RAxML web server with 1000 bootstrap  
248 replicates and the GTR+G model was selected based on Akaike information criterion  
249 (AIC) in jModeltest 2.1.7 (Darriba et al. 2012). The divergence time of DR/IR occurrence  
250 was estimated using BEAST version 1.8.2 (Suchard et al. 2018) with two fossil  
251 calibration nodes employed. A fossil calibration of the root age corresponded to the  
252 split of Lycopodiopsida and Isoetopsida (Figure 4, node A: [392-451 Ma]) (Morris et al.  
253 2018) with a selection of normal prior distributions. The other fossil calibration of the  
254 node separated Isoetaceae and Selaginellaceae (Figure 4, node B: [3722-392 Ma])  
255 (Kenrick and Crane 1997) with a lognormal prior distribution. A relaxed clock with  
256 lognormal distribution of uncorrelated rate variation was specified, and a birth-death  
257 speciation process with a random starting tree was adopted. The MCMC chain was run  
258 for 500 million generations, sampling every 1000 generations. The effective sample  
259 size (ESS) was checked in Tracer v 1.5 (Rambaut and Drummond 2009). The maximum  
260 clade credibility tree was generated using TreeAnnotator in BEAST and the tree was  
261 plotted using FigTree v. 1.4.3 (Rambaut 2017). The events of DR/IR originate,  
262 rearrangements, and DR/IR expansion/contraction in Selaginellaceae was mapped on  
263 the phylogenetic tree to explore the evolutionary trajectory of Selaginellaceae  
264 plastomes.

## 265 Results

### 266 Characteristics of Selaginellaceae Plastomes

267 The general features of twelve Selaginellaceae plastomes and four other lycophytes  
268 are summarized in Table 1 and Table S1. Compared to other lycophytes, the plastomes  
269 of Selaginellaceae showed remarkable variation in size, ranging from roughly 110 kb in  
270 *S. lyallii* to 147 kb in *S. sanguinolenta*. Size variability was partly due to the IR, which  
271 expanded to ca. 16 kb in *S. sanguinolenta* and reduced to ca. 10 kb in *S. lyallii*. Gene  
272 content was also variable in Selaginellaceae plastomes due to a number of gene losses  
273 (Table 1, Figure 1). Lycophyte plastomes generally contained 120 different genes (86  
274 protein-coding genes, 30 tRNA genes and 4 *rrn* genes), whereas it ranged from 73  
275 different genes (61 protein-coding genes, 8 tRNA genes and 4 *rrn* genes) in *S.*  
276 *tamariscina* to 102 different genes (76 protein-coding genes, 22 tRNA genes and 4 *rrn*  
277 genes) in *S. sanguinolenta*. Intron loss was detected in *atpF*, *clpP*, *rpoC1*, and *ycf3*  
278 genes. The GC content in Selaginellaceae plastomes was significantly higher than those  
279 in Isoetaceae and Lycopodiaceae. The average GC content was 53.2% in  
280 Selaginellaceae (ranging from 50.7% in *S. lyallii* to 56.5% in *S. remotifolia*) and 36.7%  
281 in other lycophytes (Table 1).

282 A noticeable plastome structure with DR was documented in *S. tamariscina* (Xu et al.  
283 2018) and *S. vardei* (Unpublished data). With our newly selected species being  
284 sequenced, we assembled the plastomes of seven species (*S. lyallii*, *S. remotifolia*, *S.*  
285 *sanguinolenta*, *S. doederleinii*, *S. moellendorffii*, *S. bisulcata*, and *S. pennata*) into the  
286 DR structure (Figure 2). Followed with the DR structure, we found that the length of  
287 two single copy regions (LSC and SSC) changed into almost equal size. However, the  
288 length of LSC (44.9 kb – 57.8 kb) was slightly shorter than that of SSC (45.3 – 62.8 kb)  
289 (Table 1), which mainly resulted from a relocation of ca. 35 kb fragments from LSC to  
290 SSC region. Only the plastomes of *S. hainanensis* and *S. uncinata* were assembled into  
291 the typical IR structure (Figure 2). We consider the assembled plastome structures as  
292 master forms in the following analyses.

## 293 **Confirmation of DR/IR Structures in Plastomes of Representative Species**

294 The DR structure in plastome of *S. vardei* for subg. *Rupestrae sensu* Weststrand and  
295 Korall (2016) (*Selaginella* sect. *Homoeophyllae sensu* Zhou and Zhang (2015)), have  
296 been confirmed by Zhang et al. (2018). The PCR confirmation of eighteen  
297 representative species with different structure (Table S2) from four subgenera *sensu*  
298 Zhou and Zhang (2015) suggested that DR structure are ubiquitous in subg.  
299 *Stachygynandrum*, subg. *Pulviniella*, subg. *Ericetorum*, and subg. *Boreoselaginella*  
300 (Figure S2 B, C, D). Particularly, the re-sequenced plastome of *S. moellendorffii* was  
301 also found to possess DR structure, which is quite inconsistent with the previously  
302 published IR structure (Smith 2009). The PCR confirmation of nine species from the  
303 same subgenus as *S. moellendorffii* further supported the DR structure (Figure S2 B).  
304 Therefore, we followed the re-sequenced DR-possessing plastome of *S. moellendorffii*  
305 for the following analyses. For subg. *Heterostachys*, the PCR confirmation of five  
306 species indicated that the IR structure only existed in the sect.  
307 *Oligomacrosporangiatae* which *S. uncinata* and *S. hainanensis* were located (Figure S2  
308 A).

## 309 **Gene/Intron Loss and Pseudogenes**

310 Gene loss or pseudogenization is a remarkable character of plastomes of  
311 Selaginellaceae including tRNA gene loss, protein-coding gene loss and intron loss.

### 312 **tRNA Gene Loss**

313 The most noticeable feature is the tRNA gene loss (Table 1, Figure 3). Plastomes in  
314 other land plants usually contain 30 different tRNA genes while Selaginellaceae  
315 plastomes have experienced an extensive tRNA gene loss and varies greatly in different  
316 lineages. Twenty-two different tRNA genes were annotated in plastome of *S.*  
317 *sanguinolenta*, whereas only eight different tRNA genes existed in *S. tamariscina*  
318 plastome. Some vestiges of tRNA genes (e.g. *trnA-UGC* exon2 and *trnI-GAU* exon1  
319 between *rrn16* and *rrn23*, *trnV-UAC* exon1 between *trnM-CAU* and *trnF-GAA*) were  
320 observed in plastome of *S. sanguinolenta*.

321 **Protein-coding Gene/Intron Loss**

322 The loss and putative pseudogenization (with internal stop codons) of protein-coding  
323 genes in Selaginellaceae plastomes are shown in figure 1, mainly focusing on NAD(P)H-  
324 dehydrogenase complex-encoding genes (*ndh* genes) and ribosomal proteins-  
325 encoding genes (*rpl/rps* genes). In *Selaginella*, the gene loss or pseudogenization of  
326 *ndh* genes occurred to a different extent. All *ndh* genes were lost in *S. vardei*, *S. indica*,  
327 and *S. lyallii*, and only one functional *ndhC* remained in *S. tamariscina*, whereas in *S.*  
328 *sanguinolenta*, four *ndh* genes (B, F, H, I) became pseudogenes, four (C, D, J, K) were  
329 completely lost, and other three (A, E, G) were still functional. The whole set of *ndh*  
330 genes in *S. bisulcata* were all pseudogenized because of internal stop codons caused  
331 by reading frame shift, whereas they were intact and functional in its sister species, *S.*  
332 *pennata*. In addition to the whole set of gene loss in specific species, several genes  
333 were lost across the whole family. The genes of *cemA*, *rpl32*, *rps15*, and *rps16* were  
334 absent in plastomes of all *Selaginella* species, whereas present in all four outgroups  
335 from *Isoetes* and *Huperzia*. The gene *accD* was non-functional (pseudogenized or lost)  
336 in all Selaginellaceae and *I. flaccida*, but was functional in Lycopodiaceae. Besides, a  
337 number of ribosomal genes (*rpl14*, 16, 20, 21, 23, 33, 36 and *rps12*, 14, 18) were lost  
338 or pseudogenized independently in different lineages of Selaginellaceae. Although  
339 *infA* is present in all bryophyte and fern lineages, it is pseudogenized in the plastomes  
340 of *I. flaccida* and *S. moellendorffii* and lost in three *Selaginella* species (*S. bisulcata*, *S.*  
341 *pennata*, and *S. tamariscina*). *MatK* gene was absent in *S. remotifolia*, *S. lyallii*, *S. indica*  
342 and *S. vardei*, and pseudogenized in *S. bisulcata*. *RpoC1* and *rpoC2* were  
343 pseudogenized in *S. bisulcata* and *rpoC1* was pseudogenized in *S. pennata*. All three  
344 *chl* genes were pseudogenized in *S. sanguinolenta*, and only *chlB* was pseudogenized  
345 in *S. vardei*. However, they were all intact in other *Selaginella* species. The gene *psaM*  
346 was non-functional (pseudogenized or lost) in all *Selaginella* species except *S.*  
347 *sanguinolenta*, which possessed an intact *psaM* gene. Another event worth noticing  
348 was the intron loss in Selaginellaceae. Two introns remained in *clpP* of *S. doederleinii*  
349 and *S. sanguinolenta*, none in *S. tamariscina*, *S. remotifolia*, *S. lyallii*, *S. indica* and *S.*

350 *vardei*, and one remained in other species of *Selaginella*. The intron of *atpF* gene was  
351 lost in *S. indica* and *S. vardei*, the intron of *rpoC1* was lost in *S. lyallii*, and the intron 2  
352 of *ycf3* gene was lost in *S. vardei*, *S. indica*, *S. lyallii* and *S. remotifolia*.

### 353 **Rearrangement Events in Plastomes of Selaginellaceae**

354 Nineteen locally collinear blocks (LCBs) (Table S5) shared by Selaginellaceae and  
355 outgroups were identified by Mauve whole plastome alignment. Each LCB for 12  
356 plastomes was numbered from 1 to 19 and assigned a  $\pm$  showing strand orientation  
357 (Table S4). The order of the 19 LCBs in each plastome was number coded for estimating  
358 breakpoint (BP) and inversions (IVs) distances between plastomes. The pairwise  
359 comparison of the two types of plastome rearrangement distances is shown in Table  
360 2. The two distances were highly correlated ( $P < 0.001$ ,  $r = 0.98$ ). Both distances were  
361 used as the estimation of the degree of genome rearrangement in the later analyses.

362 The plastome rearrangement between *I. flaccida* and *S. vardei* was described in Zhang  
363 et al. (2018). The plastomes of *S. vardei*, *S. indica*, *S. lyallii*, *S. remotifolia* and *S.*  
364 *sanguinolenta* were almost syntenic except the different extent loss of *ndh* genes  
365 (Figure 1, Figure S1) and slightly change of DR boundaries (Figure 2). Compared with  
366 the plastome of *S. sanguinolenta*, an inversion of 8 kb *psbJ-clpP* fragment (block -15, -  
367 14) was observed in the plastome of *S. tamariscina*. The *psbJ-clpP* inversion was also  
368 shared by the plastomes of *S. doederleinii* and *S. moellendorffii*, which are basically  
369 syntenic with that of *S. tamariscina*. The inversion of a ca. 20 kb *trnC-psbI* fragment  
370 (block 4, 5), absent in *S. moellendorffii* and other early diverged species, showed a  
371 derived character in the plastomes of *S. bisulcata*, *S. pennata*, *S. hainanensis*, and *S.*  
372 *uncinata*. Two extra inversions existed when comparing the plastomes of *S.*  
373 *moellendorffii* and *S. bisulcata*. The first inversion of a 9 kb *psbJ-clpP* fragment (block  
374 14, 15) was located at one end of the second inversion of 20 kb *rpl20-trnF* fragment  
375 (block -14, -13, -12) with *clpP* (block -15) being excluded. The plastome organization of  
376 *S. pennata* was basically syntenic with its sister species, *S. bisulcata*.

377 The plastomes of *S. bisulcata* and *S. pennata* were assembled into DR structure

378 whereas the plastomes of both *S. uncinata* and *S. hainanensis*, which belong to the  
379 same subgenus, retained the typical IR structure as observed in other land plants.  
380 Therefore, how the DR region change back to IR again is an intriguing phenomenon.  
381 The comparison between plastomes of *S. bisulcata* and *S. uncinata* displayed two  
382 inversions. The first inversion was a 20 kb fragment of *rpl20-trnF* (block 12, 13, 14);  
383 followed by the inversion of 65 kb fragment of *trnD-rpl20* (block 9, 10, 11, -17, -16, -  
384 15, -14, -13, -12). The first inversion occurred at one end of the second inversion. With  
385 one copy of repeat region (DR<sub>B</sub>) inside, the second inversion changed *S. uncinata*  
386 repeat regions into an IR structure. Since *S. hainanensis* is sister to *S. uncinata*, the  
387 plastome structure is basically syntenic with each other.

### 388 **Expansion and Contraction of DR/IR Regions in *Selaginella* Plastomes**

389 Repeat regions of plastomes in different lineages of *Selaginella* ranged from 10,096 bp  
390 in *S. lyallii* to 16,531 bp in *S. sanguinolenta* (Table 1). In the early diverged lineages of  
391 *S. vardei*, *S. indica*, *S. lyallii*, *S. remotifolia* and *S. sanguinolenta*, one end of the DR<sub>B</sub>  
392 region expanded and incorporated genes (*rps7*, *ndhB*, *psbM*, *petN* and *trnC*) from LSC  
393 region to a different extant, whereas the other end of the DR<sub>B</sub> region contracted to  
394 *trnN* or *trnR* (Figure 2, Figure S1). In the derived lineages like *S. tamariscina*, *S.*  
395 *doederleinii*, *S. bisulcata* and *S. hainanensis*, one end of the DR<sub>A</sub> next to the LSC region  
396 contracted to *rrn16* or *rpl23* whereas the other end of the DR<sub>A</sub> next to the SSC region  
397 expanded to include *rps4* and even one exon of *ycf3* (Figure 2, Figure S1).

### 398 **Repeats in *Selaginella* Plastomes**

399 The total number of repeats in Selaginellaceae plastomes were slightly lower than that  
400 in Isoetaceae and Lycopodiaceae plastomes, whereas repeats with the size above 50  
401 bp were mostly in Selaginellaceae plastomes (Figure 4A, Figure S2). Among the sixteen  
402 plastomes compared, *S. bisulcata* contained the most repeats (38) in lycophytes, with  
403 *S. bisulcata* and *S. pennata* possessing the most repeats above 50 bp (8), whereas *S.*  
404 *indica* had the fewest (5) in total. The number of repeats varied among the species of  
405 Selaginellaceae, and the plastomes of *S. bisulcata* and *S. pennata* contained the most

406 repeats (38 and 29) of all. The degree of plastome rearrangement estimated by BP and  
407 IV distances were moderately correlated with the total number of repeats (BP,  $P=0.034$ ,  
408  $r=0.613$ ; IVs,  $P=0.011$ ,  $r=0.702$ ) (Figure 4B, C) in all twelve *Selaginella* species, but were  
409 not correlated in the plastomes with DR structure (BP,  $P=0.498$ ; IVs,  $P=0.498$ , data not  
410 shown). We did find some repeats, which are able to mediate homologous  
411 recombination, flanking several rearrangement end points. A pair of short repeats  
412 existed at the flank of ca. 20 kb *psbI-trnC* inversion in *S. bisulcata* (48 bp) and *S.*  
413 *pennata* (60 bp) (Figure S2C, D), and another pair of repeats at the flank of 10 kb *psbJ-*  
414 *clpP* inversion in *S. doederleinii* (166 bp) and *S. moellendorffii* (264 bp) (Figure S2E, F)  
415 suggesting that repeats larger than 50 bp may have facilitated rearrangements in  
416 Selaginellaceae. Besides, a pair of ca. 1.8 kb inverted repeats exists in plastomes of *S.*  
417 *bisulcata* and *S. pennata*, and a pair of ca. 2.7 kb direct repeats exists in plastomes of  
418 *S. uncinata* and *S. hainanensis*. These two pairs of repeats, together with DR and IR,  
419 are able to frequently mediate diverse homologous recombination, and create  
420 approximately equal stoichiometric subgenomes and isomers. Therefore, both IR and  
421 DR structure exist dynamically (IR/DR coexist) in plastomes of *S. bisulcata*, *S. pennata*,  
422 *S. uncinata*, and *S. hainanensis*. (Figure 6).

### 423 **Nucleotide Substitution in *Selaginella* Plastomes**

424 The pairwise substitution rate comparison of 46 genes from single copy regions of  
425 twelve *Selaginella* plastomes showed that the dS values for the genes of DR-possessing  
426 plastomes were significantly higher than those of IR/DR-coexisting plastomes ( $P<0.01$ ),  
427 whereas the opposite trend was observed for the dN value and dN/dS ( $P<0.01$ ,  $P<0.01$ )  
428 (Figure 5). Of the 46 genes, 28 genes were inside the ca. 50 kb inversion and 18 genes  
429 were outside the inversion for DR-possessing plastomes. Comparison between genes  
430 inside and outside IV showed that dS was slightly lower in genes inside IV than outside  
431 IV without significant difference ( $P=0.042$ ), whereas the opposite trend was observed  
432 for dN and dN/dS ( $P<0.01$ ,  $P<0.01$ ) (Figure 5).

### 433 **Phylogenetic Reconstruction and Divergence Time Estimation**

434 Phylogenetic relationships of 46 protein-coding genes within Selaginellaceae were



435 basically congruent with the previously published results (Weststrand and Korall 2016a;  
436 Zhou et al. 2016) except the phylogenetic position of *S. sanguinolenta* (Figure 2).  
437 *Selaginella sanguinolenta* was placed in the second earliest diverging subg.  
438 *Boreoselaginella* and was sister to the rest of the genus except subg. *Selaginella* in  
439 Zhou et al. (2016). In Weststrand and Korall (2016a), *S. sanguinolenta* was found in two  
440 different positions (position  $\alpha$  and position  $\beta$ ), and the phylogenetic position of *S.*  
441 *sanguinolenta* in our newly reconstructed phylogeny was congruent with the position  
442  $\beta$  with 100% support. The split between Selaginellaceae and its sister family Isoetaceae  
443 occurred at 375 million years ago (Ma) (Kenrick and Crane 1997). We inferred that the  
444 occurrence time of the DR structure and the recurrence time of the IR structure  
445 (IR/DR-coexisting) was at 246 Ma and 23 Ma, respectively (Figure 2). The DR structure  
446 showed the early diverged state whereas IR structure was the derived one in the most  
447 evolved lineage in the family Selaginellaceae when mapped on the phylogenetic tree  
448 (Figure 2). The 20 kb *trnC-psbI* inversion showed a derived character for *S. pennata*, *S.*  
449 *bisulcata*, *S. hainanensis* and *S. uncinata*. The shared 9 kb *psbJ-clpP* inversion among  
450 *S. tamariscina*, *S. doederleinii*, and *S. moellendorffii* suggested their relatively close  
451 relationship (Figure 2).

452

## 453 Discussion

### 454 Gene/Intron Losses and Pseudogenes

455 Compared with *S. uncinata* (Tsuji et al. 2007) and *S. moellendorffii* (Smith 2009), the  
456 tRNA loss was even severe in the basal *Selaginella* species with only eight different  
457 tRNA genes remaining in *S. tamariscina*. However, 22 tRNA genes were annotated in  
458 the plastome of *S. sanguinolenta* (Table 1, Figure 3) with the presence of three  
459 “vestigial” tRNA genes, which were also found in *S. uncinata* plastomes (seven  
460 “vestigial” tRNA genes) (Tsuji et al. 2007). Several hypotheses have been proposed to  
461 explain why more than half of tRNA genes has been lost and how to compensate for  
462 the absence of tRNA genes from *Selaginella* plastome (Wolfe et al. 1992) (Tsuji et al.  
463 2007). The hypothesis that the lost tRNA are encoded in the nuclear genome and  
464 imported to the plastid from the cytosol, which is also known to occur for plant  
465 mitochondria, is most likely to be the explanation for the presence of “vestigial” tRNA  
466 genes found in *S. sanguinolenta* and *S. uncinata*. Furthermore, no tRNA genes were  
467 annotated in mitochondrial genome of *S. moellendorffii* (Hecht et al. 2011). Therefore,  
468 the absent tRNA genes in plastomes of *Selaginella* are most likely lost and imported  
469 from nucleus.

470 Except for the severe tRNA genes loss mentioned above, numerous protein-coding  
471 genes were also absent in *Selaginella* plastomes, especially in the species of the basal  
472 lineages (Figure 1). Five species had *ndh* gene loss to a different extent with all *ndh*  
473 genes lost in *S. vardei*, *S. indica*, and *S. lyallii*, ten lost and one (*ndhC*) intact in *S.*  
474 *tamariscina*, four lost, four pseudogenized and three intact in *S. sanguinolenta*, and 11  
475 *ndh* genes intact in other six *Selaginella* species. The gene loss of *ndh* genes have been  
476 reported in land plant plastomes many times, such as, *Najas flexilis* (Peredo et al. 2013),  
477 *Epifagus*, (Haberhausen and Zetsche 1994), *Cuscuta* (Funk et al. 2007; Logacheva et al.  
478 2011), *Neottia* (Feng et al. 2016; Haberle et al. 2008), Gnetales (Raubeson and Jansen  
479 2005), Pinaceae (Wakasugi et al. 1994), and several *Erodium* species (Blazier et al.  
480 2011b). the *ndh* genes, encoding plastid NAD(P)H-dehydrogenase complex was  
481 involved in cyclic electron flow (CEF) chain. Two independent pathways of CEF, *PGR5*-

482 dependent and *NDH*-dependent pathways, have been characterized across land plants,  
483 with the former being the main contributor in CEF (Ruhlman et al. 2015). Therefore,  
484 the *ndh* genes that were lost in different lineages of land plants were not transferred  
485 into nucleus, but most possibly replaced by the nuclear-encoded *PGR5*-dependent  
486 pathway (Ruhlman et al. 2015). The shared character in *S. vardei*, *S. indica*, *S. lyallii* and  
487 *S. tamariscina* is the extremely dry habitat and thick wax-like components on the leaf  
488 surface, likely to reflect the strong sunlight. In this case, we presume that the loss of  
489 *ndh* genes in these five species could be related to the adaptation to the dry and light-  
490 intensive habitat. The plastome of *S. sanguinolenta* could be in the intermediate phase  
491 growing in the moderate dry habitat, and the loss and pseudogenization of *ndh* genes  
492 could be a relatively recent loss. In *S. bisulcata*, all *ndh* genes become putative  
493 pseudogenes because of the internal stop codons caused by frame shift mutation,  
494 whereas all *ndh* genes are functional in the plastome of its sister species *S. pennata*  
495 (Figure 1; Figure S4). The extensive RNA editing sites in plastomes of *Selaginella* were  
496 previously reported, and the RNA editing sites could recover the pseudogenes into  
497 functional (Oldenkott et al. 2014). However, evidence from transcriptome data is  
498 necessary to elucidate whether the putative pseudogenes in *S. bisulcata* is truly  
499 deprived of function or restored after RNA editing at the transcriptome level.

500 Another noteworthy event is the intron loss in Selaginellaceae (Figure 1). The intron  
501 loss in plastomes is common in land plants (Jansen and Ruhlman 2012). Most  
502 angiosperms and ferns have two introns in *clpP* gene, whereas only one intron  
503 remained in *clpP* gene of Equisetaceae in ferns (Karol et al. 2010). In *Selaginella*,  
504 however, two introns remained in *clpP* of *S. sanguinolenta* and *S. doederleinii* as in  
505 other lycophytes (Isoetaceae and Lycopodiaceae), only one intron, similar to the  
506 plastomes of Equisetaceae, remained in *clpP* gene of other reported *Selaginella*  
507 species, and no introns existed in *clpP* of *S. tamariscina*, *S. remotifolia*, *S. lyallii*, *S.*  
508 *indica*, and *S. vardei*, similar to the plastomes of *Pinus* species (Wakasugi et al. 1994),  
509 two *Silene* species (Erixon and Oxelman 2008), and grasses (Barkan 2004; Downie and  
510 Palmer 1992). The intron of *atpF* gene was lost in *S. vardei* and *S. indica*, while the

511 intron of *rpoC1* was absent in *S. lyallii*. Besides, the intron 2 of *ycf3* gene was lost in *S.*  
512 *vardei*, *S. indica*, *S. lyallii*, and *S. remotifolia*. Observation of the intron loss in *atpF* was  
513 first uncovered in the plastome of cassava (Daniell et al. 2008) and the loss of *rpoC1*  
514 intron was found to occur multiple times in angiosperms (Downie et al. 1996). The  
515 intron 2 loss of *ycf3* genes represents the first documented case within the plastomes  
516 of land plants. In the case of intron loss, one mechanism has been proposed that  
517 involves recombination between a processed intron-less cDNA and the original intron-  
518 containing copy (Daniell et al. 2008). Under this situation, an apparent decrease of  
519 RNA editing sites in the neighboring regions of lost intron should be observed in genes  
520 losing intron. The multiple sequence alignments between intron-lost genes (*atpF*, *clpP*,  
521 *rpoC1*, and *ycf3*) and their homologues with intron from closely related species  
522 displayed apparent C to T change at the flanking regions of lost introns (Figure S5).  
523 Therefore, we propose that the intron loss of *clpP*, *atpF*, and *ycf3* in Selaginellaceae  
524 can likely be explained by this mechanism.

### 525 **Evolutionary Trajectory of DR/IR in Selaginellaceae**

526 Except the unconventional DR structure in *S. vardei* (Zhang et al., 2018) and *S.*  
527 *tamariscina* (Xu et al. 2018), we also found the DR structure existing in the plastomes  
528 of our newly sequenced seven species (*S. lyallii*, *S. remotifolia*, *S. sanguinolenta*, *S.*  
529 *tamariscina*, *S. doederleinii*, *S. moellendorffii*, *S. bisulcata*, and *S. pennata*), which  
530 showed that the DR structure in *Selaginella* plastomes is a remarkable character.  
531 However, the typical IR structure, existing in almost all land plants, still remains in the  
532 plastomes of *S. uncinata* and *S. hainanensis*. Furthermore, PCR confirmation of the  
533 plastome structure in 18 representative species from four subgenera sensu Zhou and  
534 Zhang (2015) (Table S2) showed that three subgenera in Selaginellaceae possess  
535 plastomes with DR structure, whereas in the most derived subg. *Heterostachys* the  
536 plastomes evolved into the typical IR structure again (Figure 2, Figure S3). Although  
537 the IR structure is ubiquitous in plastomes among land plants, the DR structure is  
538 indicated as the early diverged character and remained in plastomes of most lineages  
539 within Selaginellaceae (Figure 2). Given that plastomes from the other two families,

540 Lycopodiaceae and Isoetaceae, of the lycophytes possess the typical IR structure (Guo  
541 et al. 2016; Karol et al. 2010; Wolf et al. 2005; Zhang et al. 2017), we suggest that the  
542 DR structure have occurred in the Selaginellaceae plastomes after the separation from  
543 Isoetaceae (Unpublished data). The occurrence of the direction change from IR in  
544 Isoetaceae to DR in Selaginellaceae was attributed to an inversion of ca. 50 kb  
545 fragment *trnF-trnN* spanning the complete IR<sub>B</sub> region (Unpublished data). Both DR and  
546 IR structure exist in the most derived subg. *Heterostachys*, with the plastomes of *S.*  
547 *bisulcata* and *S. pennata* assembled into DR structure and the plastomes of *S. uncinata*  
548 and *S. hainanensis* assembled into IR structure. Two inversions were described  
549 between these two plastome structures, and one inversion of ca. 65 kb fragment *trnD-*  
550 *rpl20* spanning one copy of repeat region (IR<sub>B</sub>) recovered the IR structure in *S. uncinata*  
551 and *S. hainanensis* (Figure 2). Furthermore, each plastome of subg. *Heterostachys* is  
552 able to generate the IR/DR-coexisting structures owing the duplication of the large  
553 region *psbK-trnQ* (Figure 6), as is detailed discussed in the next section.

554 The result of divergence time estimation showed that the DR and IR structure (IR/DR-  
555 coexisting) occurred at about 246 Ma and 23 Ma, respectively (Figure 2). The well-  
556 known Permian-Triassic (P-T) extinction event occurred about 252 Ma ago, causing  
557 about 50% reduction in terrestrial plants diversity (McElwain and Punyasena 2007). At  
558 the P-T boundary, despite the dramatically changed terrestrial ecosystems, lycophytes,  
559 being one of the surviving plants, played a central role in repopulating the initial  
560 ecological landscape (Looy et al. 1999). Both mitochondrial and plastid genomes are  
561 more frequently subjected to alterations under specific environmental conditions  
562 (Maréchal and Brisson 2010). Given the evidence of the P-T extinction, the DR  
563 structure in Selaginellaceae is most possibly selected for better surviving the ecological  
564 upheaval (increasing anoxia, increasing aridity, and increased UV-B radiation). However,  
565 the potential mechanism for the recent recurrence of IR and the coexistence with DR  
566 structure in plastomes of Selaginellaceae need further exploration.

### 567 **Dynamic Structures of the Plastomes with DR/IR Structure of Selaginellaceae**

568 Recombination-dependent process between homologous repeats is responsible for

569 the highly dynamic structure of plant organelle genomes (plastomes and mitogenomes)  
570 (Maréchal and Brisson 2010; Ruhlman et al. 2017). Large repeats (> 1 kb) are able to  
571 mediate high frequency, reciprocal recombination intra- or intermolecularly and  
572 generally results in approximately equimolar amounts of the parental and  
573 recombinant forms (Arrieta-Montiel and Mackenzie 2011; Fauron et al. 1995). In  
574 genomes where both inverted and direct repeats are present, recombination activities  
575 in these different orientations will lead to drastically different genome organizations,  
576 containing various isomeric forms of the master chromosome and subgenomic  
577 molecules (Fauron et al. 1995).

578 The plastomes of *S. uncinata* and *S. hainanensis* were assembled into an IR structure,  
579 which we consider as master chromosome. However, another pair of ca. 2.7 kb  
580 inverted repeats spanning *psbK-trnQ* was identified in the LSC and SSC region,  
581 respectively (Figure S5). Therefore, recombination between IR generates an isomer  
582 with altered orientation of one single copy region, which, in turn, changes the inverted  
583 repeats of *psbK-trnQ* into direct (isomer I). Recombination between the copies of ca.  
584 2.7 kb inverted repeat *psbK-trnQ* could change the orientation of IR into direct (DR)  
585 and generates isomer II. Both isomer I and isomer II could give rise to two subgenomic  
586 molecules through the recombination between direct repeats, respectively (Figure 6A).

587 The plastomes of *S. bisulcata* and *S. pennata* were assembled into DR structure, which  
588 was considered as master chromosome. However, a pair of ca. 1.8 kb inverted repeats  
589 spanning *psbK-trnQ* was identified in the LSC and SSC region, respectively (Figure S5).  
590 Following the recombination activities in *S. uncinata* and *S. hainanensis*,  
591 recombination between DR gives rise to two subgenomic molecules, and  
592 recombination between the copies of ca. 1.8 kb inverted repeat *psbK-trnQ* change the  
593 orientation of DR into inverted (IR), generating isomer I. Recombination between  
594 newly created IR in isomer I generates isomer II with altered orientation of one single  
595 copy region, which similarly changes the inverted repeats of *psbK-trnQ* into direct  
596 (isomer II). Finally, recombination between the copies of direct repeat *psbK-trnQ* in  
597 isomer II also gives rise to two different subgenomic molecules (Figure 6B). Thus, these

598 frequent, reciprocal recombination activities created a dynamic complex  
599 heterogeneous population of plastomes in *S. uncinata*, *S. hainanensis*, *S. bisulcata*, and  
600 *S. pennata*.

601 However, as reported in *S. vardei* (Unpublished data), the plastomes with DR structure  
602 could only promote a master chromosome and two sets of subgenomic chromosomes  
603 at approximately equal stoichiometries by the recombination between two copies of  
604 DR within one plastome or between different molecules (Figure 6C). Either the master  
605 chromosome or subgenomic chromosomes could form head to tail concatemers of  
606 both circular and linear molecules together with branched structures through  
607 recombination between DR regions. The existence of subgenomes in species of DR-  
608 possessing plastomes have been confirmed using the PacBio reads in *S. tamariscina*  
609 (Xu et al. 2018), whereas the existence of the complex heterogeneous population of  
610 multipartite plastomes in *S. uncinata*, *S. hainanensis*, *S. bisulcata*, and *S. pennata* still  
611 need to be confirmed by long reads from PacBio or Nanopore sequencing. Considering  
612 the fact that most land plants possess plastomes with IR structure and only the early  
613 diverged lycophyte group Selaginellaceae share DR structure, plastomes with IR  
614 structure presumably have more advantageous characters for plants survival and  
615 adaptation. The coexistence of the dynamic heterogeneous plastome structures in the  
616 derived lineage is possibly in the intermediate stage, which also reached an  
617 equilibrium in plastome organization. However, the biological significance behind the  
618 diverse plastome structures, especially for adaptation to environments, and the role  
619 of nuclear-encoded, plastid-targeted genes, which control the recombination  
620 behaviors, are worth further exploration.

### 621 **Correlation between Plastome Rearrangements and Repeats in Selaginellaceae**

622 Two main forms of rearrangements, inversions and DR/IR region  
623 expansion/contraction, constitute the main rearrangement events in plastomes of  
624 Selaginellaceae. Plastome organizations of basal lineages (e.g. *S. vardej*, *S. indica*, *S.*  
625 *lyallii*, *S. remotifolia*, and *S. sanguinolenta*) of Selaginellaceae showed relatively  
626 conserved gene order, whereas rearrangements mainly existed in the more evolved

627 lineages (e.g. *S. tamariscina*, *S. doederleinii*, *S. bisulcata* and *S. uncinata*) (Figure 2;  
628 Figure S1).

629 The extensive rearrangement events in plastomes of Geraniaceae have shown to be  
630 correlated with high incidence of dispersed repetitive DNA (Weng et al. 2013). The  
631 correlation between number of repeats and the rearrangement distances was also  
632 detected in Selaginellaceae plastomes (BP,  $P=0.034$ ,  $r =0.613$ ; IVs,  $P=0.011$ ,  $r=0.702$ ,  
633 Figure 4B, C), with high frequency of repeats in IR/DR-coexisting plastomes (Figure 4A).  
634 However, no correlation was detected in the plastomes with DR structure (BP,  $P=0.498$ ,  
635  $r =-0.283$ ; IVs,  $P=0.498$ ,  $r =-0.283$ , figure not shown), suggesting that the repeats in  
636 Selaginellaceae are more associated with the structure change from DR to IR/DR  
637 coexistence. The coexistence of few repeats and DR structure in *Selaginella* plastomes,  
638 as reported in *S. vardei* and *S. indica* (Zhang et al., 2018) might have conferred an  
639 advantage to maintain the plastome stability and have been selected. On the other  
640 hand, the occurrence of repeats, especially the large one (*psbK-trnQ*), in the IR/DR-  
641 coexisting plastomes are responsible for the hypothesized dynamic plastome  
642 complexity, which has reached an equilibrium state in order to maintain stability.

#### 643 **Correlation between Plastome Rearrangements and Nucleotide Substitution Rate in** 644 **Selaginellaceae**

645 The significantly low dS value of genes of IR/DR-coexisting plastomes indicated that  
646 more efficient recombination activities, functioning as gene conversion mechanism  
647 and occurring within the single copy regions, consequently decrease the dS value in  
648 IR/DR-coexisting plastomes (Ruhlman and Jansen 2014; Ruhlman et al. 2017). However,  
649 the genes from IR/DR-coexisting plastomes exhibited accelerated dN and dN/dS  
650 compared to the genes of DR-possessing plastomes suggesting that genes in species  
651 with IR/DR-coexisting plastomes is presumably subject to much higher selective  
652 pressures, which may require fixation of functionally important mutation (Bousquet et  
653 al. 1992). For species with DR-possessing plastomes, the difference of dS between  
654 genes inside IV and outside IV was not significant ( $P= 0.042$ ), showing the 50 kb  
655 inversion causing DR structure did not have significant influence on synonymous



656 substitution rate. The significantly low  $dN$  value and  $dN/dS$  of genes outside IV is  
657 possibly correlated with the genes themselves, which usually encode the main subunit  
658 of photosynthesis-necessary proteins and under strong selection pressure (Table S6).

### 659 **Acknowledgments**

660 This work was supported by the National Natural Science Foundation of China (grant  
661 number 31670205, 31770237). The authors would like to thank Chang-Hao Li for help  
662 with data analyses, Shi-Liang Zhou, Wen-Pan Dong and Jong-Soo Kang for helpful  
663 discussions, Nawal Shrestha for helpful revision and polishing the whole manuscript.

### 664 **References**

- 665 Arrieta-Montiel MP, Mackenzie SA. 2011. Plant Mitochondrial Genomes and  
666 Recombination. In: Kempken F, editor. Plant Mitochondria. New York, NY: Springer  
667 New York. p. 65-82.
- 668 Banks JA. 2009. *Selaginella* and 400 million years of separation. *Annu Rev Plant Biol.*  
669 60: 223-238.
- 670 Barkan A. 2004. Intron splicing in plant organelles. In. *Molecular biology and*  
671 *biotechnology of plant organelles*. Dordrecht: Springer. p. 295-322.
- 672 Bernt M, et al. 2007. CREx: inferring genomic rearrangements based on common  
673 intervals. *Bioinformatics* 23.
- 674 Blazier JC, Guisinger MM, Jansen RK. 2011a. Recent loss of plastid-encoded *ndh* genes  
675 within *Erodium* (Geraniaceae). *Plant Mol Biol.* 76: 263-272.
- 676 Blazier JC, et al. 2016. Variable presence of the inverted repeat and plastome stability  
677 in *Erodium*. *Ann Bot.* 117: 1209-1220.
- 678 Bousquet J, Strauss SH, Doerksen AH, Price RA. 1992. Extensive variation in  
679 evolutionary rate of *rbcl* gene sequences among seed plants. *Proc Natl Acad Sci.*  
680 89: 7844-7848.
- 681 Braukmann TWA, Kuzmina M, Stefanović S. 2009. Loss of all plastid *ndh* genes in  
682 Gnetales and conifers: extent and evolutionary significance for the seed plant  
683 phylogeny. *Curr Genet.* 55: 323-337.
- 684 Cai Z, et al. 2008. Extensive reorganization of the plastid genome of *Trifolium*

- 685 *subterraneum* (Fabaceae) is associated with numerous repeated sequences and  
686 novel DNA insertions. *J Mol Evol.* 67: 696-704.
- 687 Castresana J. 2000. Selection of conserved blocks from multiple alignments for their  
688 use in phylogenetic analysis. *Mol Biol Evol.* 17: 540-552.
- 689 Chaw S-M, Wu C-S, Sudianto E. 2018. Evolution of gymnosperm plastid genomes. In:  
690 Chaw S-M, Jansen RK, editors. *Adv Bot Res.: Academic Press.* p. 195-222.
- 691 Daniell H, et al. 2008. The complete nucleotide sequence of the cassava (*Manihot*  
692 *esculenta*) chloroplast genome and the evolution of *atpF* in Malpighiales: RNA  
693 editing and multiple losses of a group II intron. *Theor Appl Genet.* 116: 723.
- 694 Darling AE, Mau B, Perna NT. 2010. progressiveMauve: multiple genome alignment  
695 with gene gain, loss and rearrangement. *PLoS ONE* 5: e11147.
- 696 Darriba D, Taboada GL, Doallo R, Posada D. 2012. jModelTest 2: more models, new  
697 heuristics and parallel computing. *Nat Methods* 9: 772.
- 698 Delannoy E, Fujii S, Colas des Francs-Small C, Brundrett M, Small I. 2011. Rampant gene  
699 loss in the underground orchid *Rhizanthella gardneri* highlights evolutionary  
700 constraints on plastid genomes. *Mol Biol Evol.* 28: 2077-2086.
- 701 Delsuc F, Brinkmann H, Philippe H. 2005. Phylogenomics and the reconstruction of the  
702 tree of life. *Nat Rev Genet.* 6: 361-375.
- 703 Downie SR, Llanas E, Katz-Downie DS. 1996. Multiple independent losses of the *rpoC1*  
704 intron in angiosperm chloroplast DNA's. *Syst Bot.:* 135-151.
- 705 Downie SR, Palmer JD. 1992. Use of chloroplast DNA rearrangements in reconstructing  
706 plant phylogeny. In. *Molecular systematics of plants.* Boston, MA: Springer. p. 14-  
707 35.
- 708 Erixon P, Oxelman B. 2008. Whole-gene positive selection, elevated synonymous  
709 substitution rates, duplication, and indel evolution of the chloroplast *clpP1* gene.  
710 *PLoS ONE* 3: e1386.
- 711 Fauron C, Casper M, Gao Y, Moore B. 1995. The maize mitochondrial genome: dynamic,  
712 yet functional. *Trends Genet.* 11: 228-235.
- 713 Feng Y-L, et al. 2016. Lineage-specific reductions of plastid genomes in an orchid tribe  
714 with partially and fully mycoheterotrophic species. *Gen Biol Evol.* 8: 2164-2175.

- 715 Funk HT, Berg S, Krupinska K, Maier UG, Krause K. 2007. Complete DNA sequences of  
716 the plastid genomes of two parasitic flowering plant species, *Cuscuta reflexa* and  
717 *Cuscuta gronovii*. BMC Plant Biol. 7: 45.
- 718 Gao L, et al. 2013. Plastome sequences of *Lygodium japonicum* and *Marsilea crenata*  
719 reveal the genome organization transformation from basal ferns to core  
720 leptosporangiates. Gen Biol Evol. 5: 1403-1407.
- 721 Gao L, Zhou Y, Wang Z-W, Su Y-J, Wang T. 2011. Evolution of the *rpoB-psbZ* region in  
722 fern plastid genomes: notable structural rearrangements and highly variable  
723 intergenic spacers. BMC Plant Biol. 11: 64.
- 724 Grewe F, Guo W, Gubbels EA, Hansen AK, Mower JP. 2013. Complete plastid genomes  
725 from *Ophioglossum californicum*, *Psilotum nudum*, and *Equisetum hyemale*  
726 reveal an ancestral land plant genome structure and resolve the position of  
727 Equisetales among monilophytes. BMC Evol Biol. 13: 1-16.
- 728 Gu Z, Gu L, Eils R, Schlesner M, Brors B. 2014. Circlize implements and enhances  
729 circular visualization in R. Bioinformatics 30: 2811-2812.
- 730 Guisinger MM, Kuehl JV, Boore JL, Jansen RK. 2011. Extreme reconfiguration of plastid  
731 genomes in the angiosperm family Geraniaceae: rearrangements, repeats, and  
732 codon usage. Mol Biol Evol. 28: 583-600.
- 733 Guo Z-Y, Zhang H-R, Shrestha N, Zhang X-C. 2016. Complete chloroplast genome of a  
734 valuable medicinal plant, *Huperzia serrata* (Lycopodiaceae), and comparison with  
735 its congener. Appl Plant Sci. 4: 1600071.
- 736 Haberhausen G, Zetsche K. 1994. Functional loss of all *ndh* genes in an otherwise  
737 relatively unaltered plastid genome of the holoparasitic flowering plant *Cuscuta*  
738 *reflexa*. Plant Mol Biol. 24: 217-222.
- 739 Haberle RC, Fourcade HM, Boore JL, Jansen RK. 2008. Extensive rearrangements in the  
740 chloroplast genome of *Trachelium caeruleum* are associated with repeats and  
741 tRNA genes. J Mol Evol. 66: 350-361.
- 742 Hecht J, Grewe F, Knoop V. 2011. Extreme RNA editing in coding islands and abundant  
743 microsatellites in repeat sequences of *Selaginella moellendorffii* mitochondria:  
744 the root of frequent plant mtDNA recombination in early tracheophytes. Gen Biol

- 745           Evol. 3: 344-358.
- 746 Jansen RK, et al. 2007. Analysis of 81 genes from 64 plastid genomes resolves  
747           relationships in angiosperms and identifies genome-scale evolutionary patterns.  
748           Proc Natl Acad Sci. 104: 19369-19374.
- 749 Jansen RK, Ruhlman TA. 2012. Plastid genomes of seed plants. In: Bock R, Knoop V,  
750           editors. Genomics of Chloroplasts and Mitochondria. Dordrecht: Springer  
751           Netherlands. p. 103-126.
- 752 Jermy AC. 1990. Selaginellaceae. In: In: Kramer K, Green PS, editors. The Families and  
753           Genera of the Vascular Plants I: Pteridophytes and Gymnosperms: Springer Berlin  
754           Heidelberg. p. 39-45.
- 755 Jermy AC. 1986. Subgeneric names in *Selaginella*. Fern Gaz. 13: 117-118.
- 756 Jin J-J, et al. 2018. GetOrganelle: a simple and fast pipeline for de novo assembly of a  
757           complete circular chloroplast genome using genome skimming data. bioRxiv:  
758           256479.
- 759 Karol KG, et al. 2010. Complete plastome sequences of *Equisetum arvense* and *Isoetes*  
760           *flaccida*: implications for phylogeny and plastid genome evolution of early land  
761           plant lineages. BMC Evol Biol. 10: 1-16.
- 762 Katoh K, Standley DM. 2013. MAFFT multiple sequence alignment software version 7:  
763           improvements in performance and usability. Mol Biol Evol. 30: 772-780.
- 764 Kearse M, et al. 2012. Geneious Basic: an integrated and extendable desktop software  
765           platform for the organization and analysis of sequence data. Bioinformatics 28:  
766           1647-1649.
- 767 Kenrick P, Crane PR. 1997. The origin and early diversification of land plants: A cladistic  
768           study. Smithsonian Institution Press Washington DC.
- 769 Laslett D, Canback B. 2004. ARAGORN, a program to detect tRNA genes and tmRNA  
770           genes in nucleotide sequences. Nucleic Acids Res. 32: 11-16.
- 771 Lavin M, Doyle JJ, Palmer JD. 1990. Evolutionary significance of the loss of the  
772           chloroplast - DNA inverted repeat in the Leguminosae subfamily Papilionoideae.  
773           Evolution 44: 390-402.
- 774 Li J, Wang S, Yu J, Wang L, Zhou S. 2013. A modified CTAB protocol for plant DNA

- 775 extraction. *Bulletin of Botany* 48: 72-78.
- 776 Logacheva MD, Schelkunov MI, Penin AA. 2011. Sequencing and analysis of plastid  
777 genome in mycoheterotrophic orchid *Neottia nidus-avis*. *Gen Biol Evol.* 3: 1296-  
778 1303.
- 779 Looy CV, Brugman WA, Dilcher DL, Visscher H. 1999. The delayed resurgence of  
780 equatorial forests after the Permian–Triassic ecologic crisis. *Proc Natl Acad Sci.* 96:  
781 13857-13862.
- 782 Maréchal A, Brisson N. 2010. Recombination and the maintenance of plant organelle  
783 genome stability. *New Phytol.* 186: 299-317.
- 784 McElwain JC, Punyasena SW. 2007. Mass extinction events and the plant fossil record.  
785 *Trends Ecol Evol.* 22: 548-557.
- 786 Morris JL, et al. 2018. The timescale of early land plant evolution. *Proc Natl Acad Sci.*  
787 115: E2274.
- 788 Mower JP, Vickrey TL. 2018. Structural diversity among plastid genomes of land plants.  
789 In: Chaw S-M, Jansen RK, editors. *Adv Bot Res.*: Academic Press. p. 263-292.
- 790 Oldenburg DJ, Bendich AJ. 2015. DNA maintenance in plastids and mitochondria of  
791 plants. *Frontiers in Plant Science* 6.
- 792 Oldenkott B, Yamaguchi K, Tsuji-Tsukinoki S, Knie N, Knoop V. 2014. Chloroplast RNA  
793 editing going extreme: more than 3400 events of C-to-U editing in the chloroplast  
794 transcriptome of the lycophyte *Selaginella uncinata*. *RNA* 20: 1499-1506.
- 795 Peredo EL, King UM, Les DH. 2013. The plastid genome of *Najas flexilis*: adaptation to  
796 submersed environments is accompanied by the complete loss of the NDH  
797 complex in an aquatic angiosperm. *PLoS ONE* 8: e68591.
- 798 Rambaut A. 2017. FigTree-version 1.4. 3, a graphical viewer of phylogenetic trees. In.  
799 Rambaut A, Drummond A. 2009. *Tracer: MCMC trace analysis tool, version 1.5.*  
800 University of Oxford: Oxford.
- 801 Raubeson LA, Jansen RK. 1992. Chloroplast DNA evidence on the ancient evolutionary  
802 split in vascular land plants. *Science* 255: 1697-1699.
- 803 Raubeson LA, Jansen RK. 2005. Chloroplast genomes of plants. In. *Plant diversity and*  
804 *evolution: genotypic and phenotypic variation in higher plants*: CABI Publishing.

805 p. 45-68.

806 Ruhlman TA, et al. 2015. NDH expression marks major transitions in plant evolution  
807 and reveals coordinate intracellular gene loss. *BMC Plant Biol.* 15: 100.

808 Ruhlman TA, Jansen RK. 2018. Aberration or analogy? The atypical plastomes of  
809 Geraniaceae. In: Chaw S-M, Jansen RK, editors. *Adv Bot Res.*: Academic Press. p.  
810 223-262.

811 Ruhlman TA, Jansen RK. 2014. The plastid genomes of flowering plants. *Chloroplast  
812 biotechnology: Methods and protocols*: 3-38.

813 Ruhlman TA, Zhang J, Blazier JC, Sabir JS, Jansen RK. 2017. Recombination-dependent  
814 replication and gene conversion homogenize repeat sequences and diversify  
815 plastid genome structure. *Am J Bot.* 104: 559-572.

816 Sanderson MJ, et al. 2015. Exceptional reduction of the plastid genome of saguaro  
817 cactus (*Carnegiea gigantea*): Loss of the *ndh* gene suite and inverted repeat. *Am  
818 J Bot.* 102: 1115-1127.

819 Smith DR. 2009. Unparalleled GC content in the plastid DNA of *Selaginella*. *Plant Mol  
820 Biol.* 71: 627-639.

821 Suchard MA, et al. 2018. Bayesian phylogenetic and phylodynamic data integration  
822 using BEAST 1.10. *Virus Evolution* 4: vey016.

823 Tamura K, Dudley J, Nei M, Kumar S. 2007. MEGA4: molecular evolutionary genetics  
824 analysis (MEGA) software version 4.0. *Mol Biol Evol.* 24: 1596-1599.

825 Tsuji S, et al. 2007. The chloroplast genome from a lycophyte (microphylophyte),  
826 *Selaginella uncinata*, has a unique inversion, transpositions and many gene losses.  
827 *J Plant Res.* 120: 281-290.

828 Volfovsky N, Haas BJ, Salzberg SL. 2001. A clustering method for repeat analysis in DNA  
829 sequences. *Genome Biol.* 2: 1-11.

830 Wakasugi T, et al. 1994. Loss of all *ndh* genes as determined by sequencing the entire  
831 chloroplast genome of the black pine *Pinus thunbergii*. *Proc Natl Acad Sci.* 91:  
832 9794-9798.

833 Weng M-L, Blazier JC, Govindu M, Jansen RK. 2013. Reconstruction of the ancestral  
834 plastid genome in Geraniaceae reveals a correlation between genome

- 835 rearrangements, repeats and nucleotide substitution rates. *Mol Biol Evol.* 31:  
836 645-659.
- 837 Weststrand S, Korall P. 2016a. Phylogeny of Selaginellaceae: There is value in  
838 morphology after all! *Am J Bot.* 103: 2136-2159.
- 839 Weststrand S, Korall P. 2016b. A subgeneric classification of *Selaginella*  
840 (Selaginellaceae). *Am J Bot.* 103: 2160-2169.
- 841 Wick RR, Schultz MB, Zobel J, Holt KE. 2015. Bandage: interactive visualization of de  
842 novo genome assemblies. *Bioinformatics* 31: 3350-3352.
- 843 Wicke S, Schäferhoff B, dePamphilis CW, Müller KF. 2013. Disproportional plastome-  
844 wide increase of substitution rates and relaxed purifying selection in genes of  
845 carnivorous Lentibulariaceae. *Mol Biol Evol.* 31: 529-545.
- 846 Wicke S, Schneeweiss GM, dePamphilis CW, Müller KF, Quandt D. 2011. The evolution  
847 of the plastid chromosome in land plants: gene content, gene order, gene  
848 function. *Plant Mol Biol.* 76: 273-297.
- 849 Wolf PG, et al. 2005. The first complete chloroplast genome sequence of a lycophyte,  
850 *Huperzia lucidula* (Lycopodiaceae). *Gene* 350: 117-128.
- 851 Wolfe KH, Mordent CW, Ems SC, Palmer JD. 1992. Rapid evolution of the plastid  
852 translational apparatus in a nonphotosynthetic plant: loss or accelerated  
853 sequence evolution of tRNA and ribosomal protein genes. *J Mol Evol.* 35: 304-317.
- 854 Wu C-S, Chaw S-M. 2015. Evolutionary stasis in cycad plastomes and the first case of  
855 plastome GC-biased gene conversion. *Gen Biol Evol.* 7: 2000-2009.
- 856 Xu Z, et al. 2018. Genome analysis of the ancient tracheophyte *Selaginella tamariscina*  
857 reveals evolutionary features relevant to the acquisition of desiccation tolerance.  
858 *Molecular Plant* 11: 983-994.
- 859 Yang Z. 2007. PAML 4: phylogenetic analysis by maximum likelihood. *Mol Biol Evol.* 24:  
860 1586-1591.
- 861 Zhang H-R, Kang J-S, Viane RL, Zhang X-C. 2017. The complete chloroplast genome  
862 sequence of *Huperzia javanica* (sw.) CY Yang in Lycopodiaceae. *Mitochondrial*  
863 *DNA Part B* 2: 216-218.
- 864 Zhang XC, Nootboom HP, Kato M. 2013. Selaginellaceae. In: Wu ZY, Raven PH, Hong

865 DY, editors. Flora of China: Science Press, Beijing and Missouri Botanical Garden  
866 Press, St. Louis,. p. 37-66.

867 Zhou X-M, et al. 2016. A large-scale phylogeny of the lycophyte genus *Selaginella*  
868 (*Selaginellaceae*: *Lycopodiopsida*) based on plastid and nuclear loci. *Cladistics* 32:  
869 360-389.

870 Zhou X-M, Zhang L-B. 2015. A classification of *Selaginella* (*Selaginellaceae*) based on  
871 molecular (chloroplast and nuclear), macromorphological, and spore features.  
872 *Taxon* 64: 1117-1140.

873



874 **Figure legends**

875 **Figure 1. Protein-coding genes in Selaginellaceae and other lycophytes.** Intact genes  
876 per species are indicated by black boxes, dark grey box represent putative  
877 pseudogenes, light grey and white boxes mark intron and gene losses, respectively.  
878 PEP—plastid-encoded RNA polymerase.

879 **Figure 2. Phylogeny reconstruction and time divergence estimation of lycophytes**  
880 **with plastome rearrangement events mapped on the branches.** Node A-B represent  
881 the calibration nodes. Node A: fossil calibration of the root age corresponding to the  
882 split of Lycopodiopsida and Isoetopsida (392-451 Ma); node B: fossil node separating  
883 Selaginellaceae and its sister family Isoetaceae (372-392 Ma). Black star represents the  
884 occurrence time of plastomes with DR structure, and grey star represents the  
885 occurrence time of plastomes with IR/DR-coexisting structure.

886 **Figure 3. tRNA genes in Selaginellaceae and other lycophytes.** Black box represents  
887 tRNA genes with two copies, grey box represents tRNA genes with one copy, and white  
888 box represents tRNA gene loss.

889 **Figure 4. Statistics of repeat analyses in Selaginellaceae. a,** The number of different  
890 size repeats; **b,** Correlation of BP distance with the number of repeats; **c,** Correlation  
891 of IV distance with the number of repeats.

892 **Figure 5. Nucleotide substitution rate analyses in Selaginellaceae. a,** Substitution rate  
893 of genes from DR-possessing plastomes and IR/DR-coexisting plastomes; **b,**  
894 Substitution rate of genes inside IV and outside IV from DR-possessing plastomes.

895 **Figure 6. Dynamic structures of plastomes with DR/IR structure of Selaginellaceae.**  
896 **a,** Recombination activities between repeats in plastomes of *S. uncinata* and *S.*  
897 *hainanensis*. The red and green block represents two copies of IR with arrows at the  
898 end showing orientation and the short orange blocks represent two copies of repeats  
899 (*psbK-trnQ*). The black double arrows show recombination between IR and the orange  
900 double arrows show recombination between repeats *psbK-trnQ*; **b,** Recombination  
901 activities between repeats in plastomes of *S. bisulcata* and *S. pennata*. The red and

902 green blocks represent two copies of DR with arrows at the end showing orientation  
903 and the short orange blocks represent two copies of repeats (*psbK-trnQ*). The black  
904 double arrows show recombination between DR and the orange double arrows show  
905 recombination between repeats *psbK-trnQ*; **c**, Recombination activities between  
906 repeats in plastomes with DR structure.

907

908

909

Table 1 Plastome Characteristics for Representative Selaginellaceae in Comparison to Four Lycophytes

Species	Size (bp)	LSC (bp)	SSC (bp)	IR (bp)	No. different genes	No. different protein-coding genes (duplicated)	No. different tRNA genes (duplicated)	No. different rRNA genes (duplicated)	GC content (%)
<i>S. uncinata</i>	144,161	77,752	40,851	12,779	97	81 (3)	12 (3)	4 (4)	54.9
<i>S. hainanensis</i>	144,201	77,780	40,819	12,801	97	81 (3)	12 (3)	4 (4)	54.8
<i>S. bisulcata</i>	140,509	55,598	59,659	12,626	94	78 (3)	12 (3)	4 (4)	52.8
<i>S. pennata</i>	138,024	54,979	59,847	11,599	90	77 (3)	9 (2)	4 (4)	52.9
<i>S. moellendorffii</i>	143,525	58,198	61,129	12,099	96	78 (1)	14 (2)	4 (4)	51
<i>S. doederleinii</i>	142,752	57,841	62,865	11,023	96	78 (1)	14 (2)	4 (4)	51.1
<i>S. tamariscina</i>	126,700	53,299	47,741	12,830	73	61 (1)	8 (1)	4 (4)	54.1
<i>S. sanguinolenta</i>	147,148	54,436	59,650	16,531	102	76 (4)	22 (3)	4 (4)	50.8
<i>S. remotifolia</i>	131,866	46,351	55,851	14,832	87	71 (3)	12 (2)	4 (4)	56.5
<i>S. lyallii</i>	110,411	44,943	45,276	10,096	76	60 (1)	13 (2)	4 (4)	50.7
<i>S. indica</i>	122,460	45,711	48,395	14,177	78	62 (3)	12(3)	4 (4)	53.6
<i>S. vardei</i>	121,254	45,792	47,676	13,893	78	62 (3)	12(3)	4 (4)	53.2
<i>I. flaccida</i>	145,303	91,862	27,275	13,118	123	87 (3)	32 (5)	4 (4)	37.9
<i>H. javanic</i>	154,415	104,120	19,667	15,314	119	86 (3)	29 (4)	4 (4)	36.4
<i>H. lucidula</i>	154,373	104,088	19,657	15,314	119	86 (3)	29 (4)	4 (4)	36.2
<i>H. serrata</i>	154,176	104,080	19,658	12,219	120	86 (3)	30 (5)	4 (4)	36.3

Table 2. Pairwise Comparison of Genome Rearrangement Distances.

	Hs	If	Sv	Si	Sr	Sl	Ss	St	Sd	Sm	Sp	Sb	Su	Sh
<i>H. serrata</i>	-													
<i>I. flaccida</i>	8/6	-												
<i>S. vardei</i>	5/3	10/8	-											
<i>S. indica</i>	5/3	10/8	0/0	-										
<i>S. remotifolia</i>	5/3	10/8	3/4	3/4	-									
<i>S. lyallii</i>	5/3	10/8	3/4	3/4	0/0	-								
<i>S. sanguinolenta</i>	5/3	10/8	3/4	3/4	0/0	0/0	-							
<i>S. tamariscina</i>	4/2	11/8	5/4	5/4	5/4	5/4	5/4	-						
<i>S. doederleinii</i>	4/2	11/8	5/4	5/4	5/4	5/4	5/4	0/0	-					
<i>S. moellendorffii</i>	4/2	11/8	5/4	5/4	5/4	5/4	5/4	0/0	0/0	-				
<i>S. pennata</i>	6/5	13/11	7/6	7/6	7/6	7/6	7/6	7/5	7/5	7/5	-			
<i>S. bisulcata</i>	6/5	13/11	7/6	7/6	7/6	7/6	7/6	7/5	7/5	7/5	0/0	-		
<i>S. uncinata</i>	6/5	12/10	7/6	7/6	7/6	7/6	7/6	7/5	7/5	7/5	3/2	3/2	-	
<i>S. hainanensis</i>	6/5	12/10	7/6	7/6	7/6	7/6	7/6	7/5	7/5	7/5	3/2	3/2	0/0	-

NOTE.—The lower diagonal refers to BP/IV distance.

1 **Supplementary Material**

2 **Figure S1. Detailed plastid genome structures of Lycophyte species.** HL, *Huperzia*  
3 *lucidula*; HS, *H. serrata*; HJ, *H. javanica*; IF, *Isoetes flaccida*; SV, *Selaginella vardei*; SI,  
4 *S. indica*; SL, *S. lyallii*; SR, *S. remotifolia*; SS, *S. sanguinolenta*; ST, *S. tamariscina*; SD, *S.*  
5 *doederleinii*; SM, *S. moellendorffii*; SP, *S. pennata*; SB, *S. bisulcata*; SU, *S. uncinata*; SH,  
6 *S. hainanensis*. Genes are colored by function. Black star marks the occurrence of DR  
7 structure, grey star marks the occurrence of IR/DR-coexisting structure in  
8 Selaginellaceae. Orange arrows in DR/IR region of plastomes show the contraction and  
9 expansion.

10 **Figure S2 PCR gels of the representative species in subgenera.** a, species from subg.  
11 *Heterstachys*. **8203**, *S. helferi*; **7833**, *S. picta*; **2415**, *S. mairei*; **7187**, *S. delicatula*; **6548**,  
12 *S. willdenowii*. **1**, *ycf2-ndhJ*; **2**, *rpl2-rpl23*; **3**, *ycf3-rps4*; **4**, *trnD-petN*; **5**, *ndhF-rps4*; **6**,  
13 *rpl2-rps7*. b, species from subg. *Stachygynandrum*. **7867**, *S. commutata*; **7899**, *S.*  
14 *guihaia*; **7895**, *S. rolandiprincipis*; **8176**, *S. scabrifolia*; **7863**, *S. biformis*; **7643**, *S. davidii*;  
15 **8201**, *S. erythropus*; **2016015**, *S. gebauriana*; **6050**, *S. involvens*. **1**, *ycf3-rps4*; **2**, *rrn16-*  
16 *rpl23*; **3**, *trnF-chlL*; **4**, *ndhF-rps4*; **5**, *rrn16-rps7*. c, species from subg. *Pulviniela*. **519**, *S.*  
17 *pulvinata*; **7644**, *S. stauntoniana*. **1**, *ycf3-ycf3*; **2**, *rrn16-rpl23*; **3**, *ndhC-chlL*; **4**, *ccsA-ycf3*;  
18 **5**, *rrn16-rps7*. d, species from subg. *Boreoselaginella*. **179**, *S. nummularifolia*; **7833**, *S.*  
19 *rossii*. **1**, *rps4-rrn5*; **2**, *ndhB-rpl2*; **3**, *trnF-chlL*; **4**, *ndhF-rrn5*; **5**, *trnL-trnC*.

20 **Figure S3 Comparisons of *ndh* genes between *S. bisulcata* and *S. pennata*.**

21 **Figure S4 Comparisons of intron-loss genes among closely related species.**

22 **Figure S5. Distribution of repeats in plastomes of newly sequenced *Selaginella***  
23 **species.**

24 **Supplementary tables:**

25 Table S1. Technical details of the Illumina datasets and genome assemblies.

26 Table S2 PCR confirmation for plastomes structure of representative species of four  
27 genera.

28 Table S3. Primers newly designed for PCR amplifications of the sampled representative  
29 species of the five main lineages in Selaginellaceae.

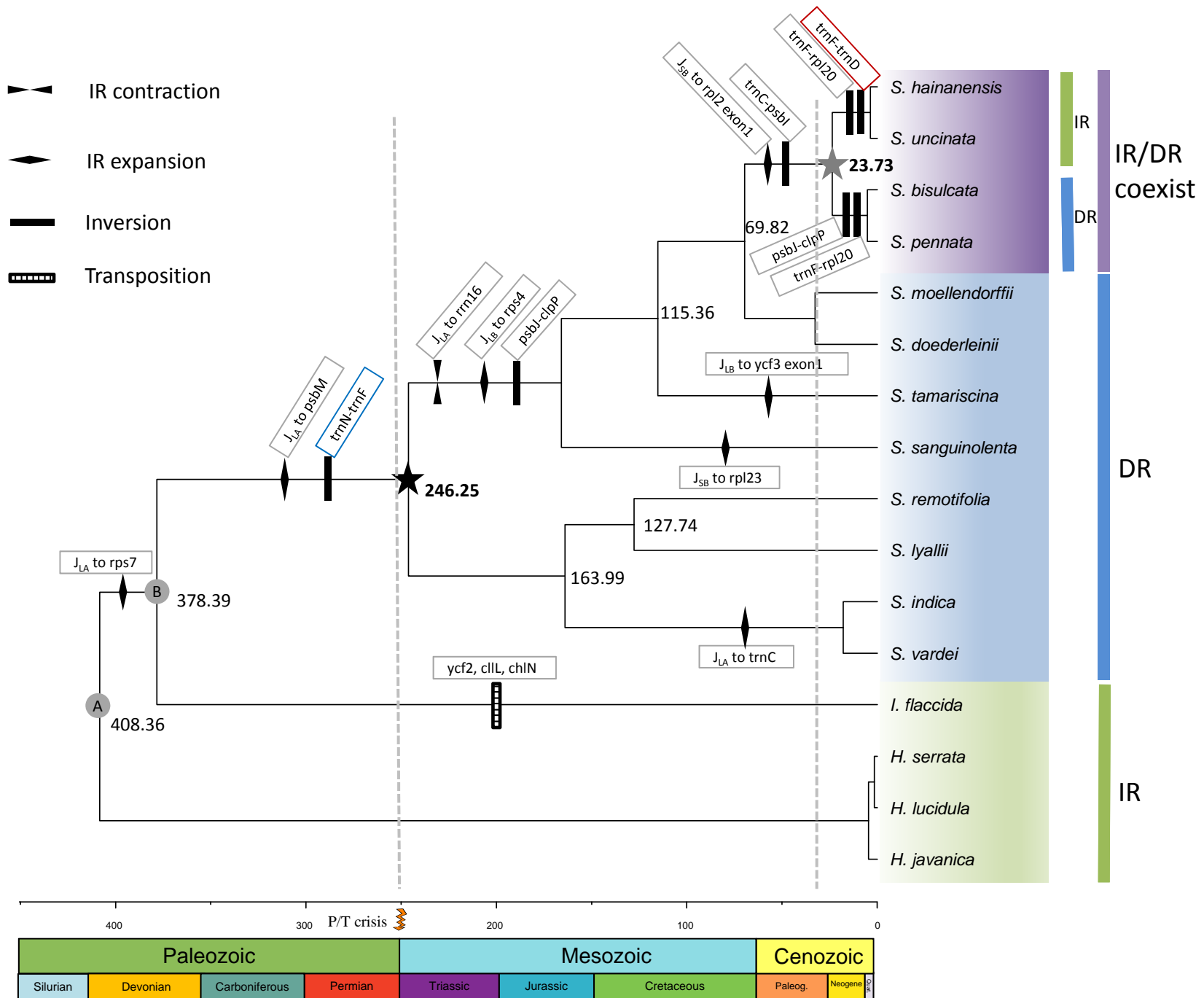
30 Table S4. The permutation of number coded Locally Collinear Block (LCB) for each  
31 plastome. Negative number indicates an inversion of the given LCB.

32 Table S5. Locally Collinear Blocks identified by Mauve alignment of 12 plastomes of  
33 lycophytes.

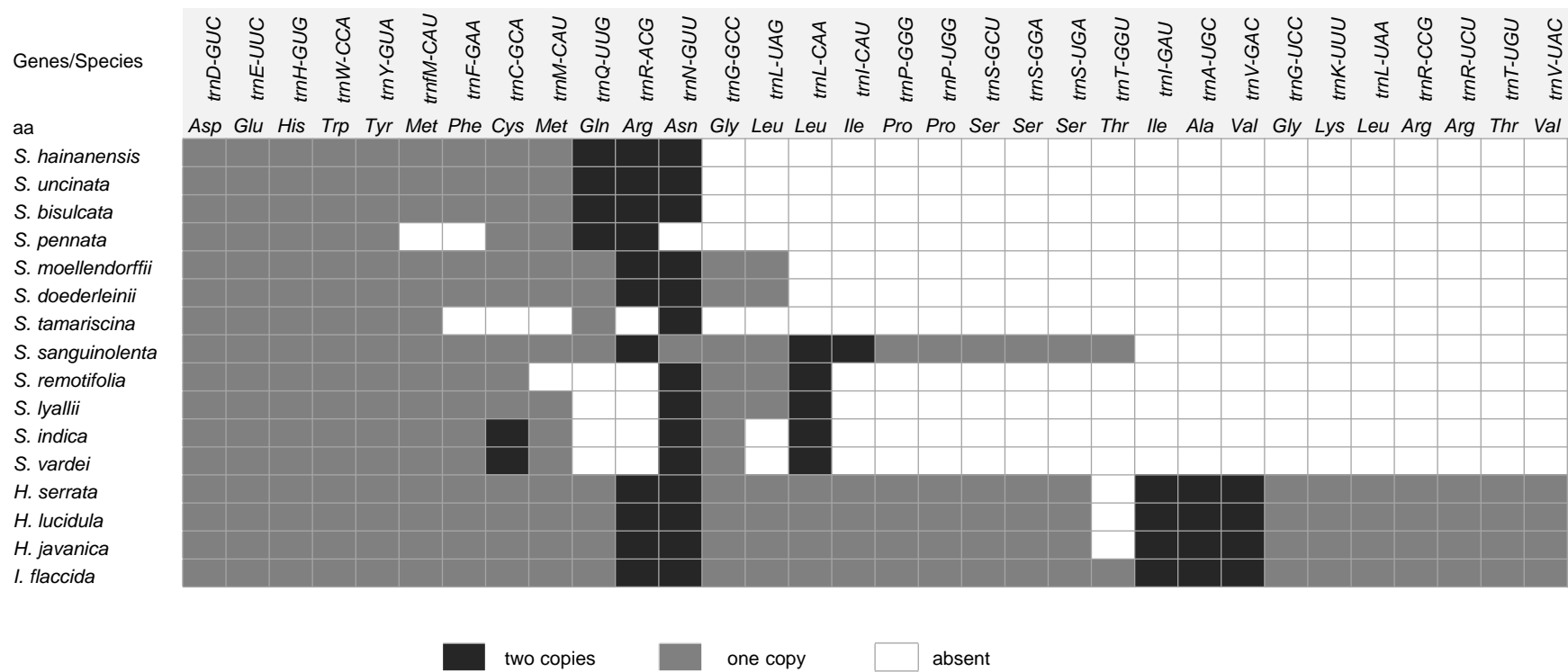
34 Table S6. Genes inside and outside ca. 50 kb inversion of plastomes with DR structure.

35









two copies
  one copy
  absent

